JACS
JOURNAL OF THE AMERICAN CHEMICAL SOCIETY
Article
pubs.acs.org/JACS

Healable Luminescent Self-Assembly Supramolecular Metallogels Possessing Lanthanide (Eu/Tb) Dependent Rheological and Morphological Properties

Miguel Martínez-Calvo,[†,∥,⊥] Oxana Kotova,[†,⊥] Matthias E. Möbius,[‡] Alan P. Bell,[§] Thomas McCabe,[†] John J. Boland,[§] and Thorfinnur Gunnlaugsson*[,†]

[†]School of Chemistry and Trinity Biomedical Sciences Institute (TBSI), Trinity College Dublin, University of Dublin, 152-160 Pearse Street, Dublin 2, Ireland

[‡]Sami Nasr Institute of Advanced Materials (SNIAM), School of Physics, Trinity College Dublin, University of Dublin, Dublin 2, Ireland

[§]Centre for Research on Adaptive Nanostructures and Nanodevices (CRANN) and School of Chemistry, Trinity College Dublin, University of Dublin, Dublin 2, Ireland

Supporting Information

ABSTRACT: Herein we present the use of lanthanide directed self-assembly formation (Ln(III) = Eu(III), Tb(III)) in the generation of luminescent supramolecular polymers, that when swelled with methanol give rise to self-healing supramolecular gels. These were analyzed by using luminescent and ^{1}H NMR titrations studies, allowing for the identification of the various species involved in the subsequent Ln(III)-gel formation. These highly luminescent gels could be mixed to give a variety of luminescent colors depending on their Eu(III):Tb(III) stoichiometric ratios. Imaging and rheological studies showed that these gels prepared using only Eu(III) or only Tb(III) have different morphological and rheological properties, that are also different from those determined upon forming gels by mixing of Eu(III) and Tb(III) gels. Hence, our results demonstrate for the first time the crucial role the lanthanide ions play in the supramolecular polymerization process, which is in principle a host−guest interaction, and consequently in the self-healing properties of the corresponding gels, which are dictated by the same host−guest interactions.

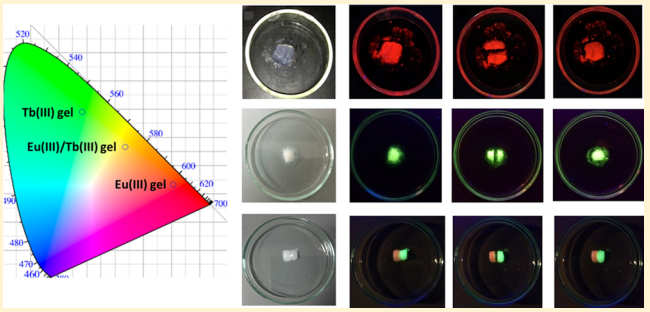

INTRODUCTION

Supramolecular self-assembly formation of soft materials such as gels have attracted the attention of researchers across various disciplines due to the rich potential they can provide within different fields of applications.[1−4] The formation of such materials is controlled by the interplay of self-complementary and intermolecular supramolecular interactions; these are further enforced through the generation of a multidimensional matrix structure.[5−8] This makes the design of new classes of small molecules that can give rise to gelation with targeted properties often highly challenging as minor modifications can greatly affect the macroscopic properties of the resulting material in an unexpected manner. To date, the generation of soft matter has been somewhat dominated by the use of organic gelators which have been mainly serendipitously discovered. However, recently the concept of multicomponent supramolecular gels has been introduced, where, for instance, ions in conjunction with gelators based on metal coordinating ligands[9] have been used in order to gain better control over structure (and hence, morphology), physical properties, and applications, *etc.*, of such soft materials.[9−11] This concept has recently been elegantly demonstrated by Steed, Maitra, Rowan, Yam, De Cola, and co-workers,[12−16] to name just a few. In recent work we have generated luminescent supramolecular gels by combining classical self-assembly concepts (such as hydrogen bonding and $\pi-\pi$ interactions) with metal coordination, by employing ligands that can bind to lanthanides (Ln) and transition metal ions. Using lanthanide ions, themselves possessing unique and highly desirable physical properties,[17] we have demonstrated the formation of luminescent metallogels, where the coordination of ions such as Eu(III) not only gives rise to unique luminescent properties, but also, due to high coordination requirements of the Eu(III) ions, aids in the formation of 3D structures with mechanically enforced properties not seen for corresponding organogels (i.e., in the absence of the ions).[18] We also showed that, upon aging, these metallo(hydro)gels could be used as a platform for growing unique nanostructures, not previously seen, such as NaCl and KCl nanowires.[19] The concept of self-healing of soft matter is a

Received: November 25, 2014
Published: January 15, 2015

DOI: 10.1021/ja511799n
J. Am. Chem. Soc. 2015, 137, 1983−1992

Scheme 1. Self-Assembly Formation of (A) Ln:H_2L with the Following Formation of Higher Order Metallo-Supramolecular Polymers (B, C) with Structural Formula of H_2L

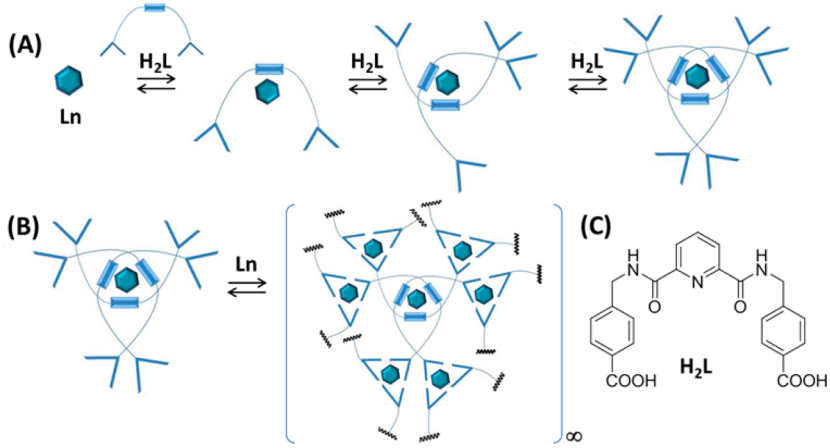

current topical area of research within supramolecular chemistry.[14,20−22] Through the use of molecular recognition strategies (e.g., host−guest chemistry), self-healing supramolecular polymers and gels have recently been formed and studied.[23,24] Capitalizing on the luminescent properties of the lanthanides within supramolecular architectures has been of particular interest to our research endeavor.[25−28] With this in mind, we set out to explore the potential of using lanthanide ions as "guests" in the generation of such self-healing soft matter in combination with structurally simple and robust organic polydentate ligands, functioning as "hosts". As alluded to above, the lanthanides have unique physical properties stemming from the f-electrons.[17] Generally, Eu(III) and Tb(III) will have similar coordination properties, while properties such as luminescent efficiency, lifetimes, *etc.* can vary between complexes formed from the same ligands.[29,30] Furthermore, we, and others, have demonstrated that the stability constant for the formation of ternary complexes involving these ions can often differ.[31,32] We thus proposed that these affinity differences could potentially be exploited with a view of modulating the properties of metallo-supramolecular polymers and metallogels such as their morphology and rheology. Herein, we show that such a design strategy is achievable, using the pyridine-2,6-dicarboxylic acid (**H_2dpa**) derivative **H_2L** (4,4′-(((pyridine-2,6-dicarbonyl)bis-(azanediyl))bis(methylene))-dibenzoic acid), Scheme 1 and Supporting Information. The ligand was designed to facilitate the initial formation of three-dimensional self-assembly units in either 1:2 or 1:3 (**Ln:H_2L**) stoichiometries; in the past we[31] and others[32−35] have demonstrated the self-assembly of such **H_2dpa** ligands into luminescent "bundles". We foresaw that these initial **Ln:H_2L** stochiometries would then form larger self-assemblies through the formation of higher order metallo-supramolecular polymers or gels by cross-linking of the initially preorganized complexes (via the terminal *para* carboxylic acids groups) upon addition of further equivalents of **Ln**.

We demonstrate that such gels can be formed reproducibly and are luminescent (giving rise to red (Eu(III)) or green (Tb(III)) emission depending of the lanthanide ion used), and possess self-healing properties. Moreover, we show that the mechanical mixing of the same volumes of these two lanthanide gels results in the formation of a mixed gel with orange emission, which can also self-heal, possessing unexpectedly different rheological properties compared to "pure" Eu(III) and Tb(III) gels indicating that the self-recognition processes in the individual gels is different from that of the mixed systems.

RESULTS AND DISCUSSION

Synthesis and Structural Characterization of H_2L and Its Corresponding Eu(III) and Tb(III) Complexes. The synthesis of ligand **H_2L** was performed in three steps from commercially available 4-(aminomethyl)benzoic acid **1** (see Supporting Information), by converting it into the ester **2** and coupling the resulting product with 2,6-pyridine-dicarboxylic acid **3** in 2:1 stoichiometry. Base hydrolysis of the protected **4** followed by adjusting the pH to 2, resulting in the formation of **H_2L** in 82% yield, which was fully characterized (see Supporting Information). X-ray quality crystalline prisms were also obtained by slow evaporation of **H_2L** from ethanol under ambient conditions, which further confirmed the formation of the desired product. The long-range interactions in solid state consisted of both intermolecular and intramolecular hydrogen bonding as well as $\pi-\pi$ stacking interactions (see Supporting Information).[36,37] Thermogravimetric analysis (TGA) on **H_2L** (see Supporting Information) showed a weight loss, assigned to loss of water molecules form the solid sample of **H_2L**, which occurred until ∼100 °C after which the compound remained stable until 260 °C, at which temperature a decomposition started. The reaction of **H_2L** with $Ln(CF_3SO_3)_3$ (Ln = Eu, Tb) in 3:1 stoichiometry in methanol solution under microwave irradiation (75 °C, 20 min) resulted in the formation of lanthanide complexes $Ln(\mathbf{H_2L})_n$ (where Ln = Eu or Tb; n = 2.50 and 2.05, respectively) as white powders after precipitation out of CH_3OH using diethyl ether diffusion (see Supporting Information). The overall quantum yield of the lanthanide-centered luminescence obtained for both Ln(III) complexes in methanol upon the ligand excitation (Φ_L^{Ln}, %) is 4.9 ± 0.1% for the Eu(III) complex and 7.2 ± 0.5% for the Tb(III) one.[38]

The hydration state (the number of metal-bound water molecules or the q-value) of both complexes was determined by recording the lanthanide centered excited state lifetimes in both H_2O and D_2O, respectively, upon excitation at 275 nm.[39] In the case of Eu(III) the excited state decay was best fitted to biexponential decay (H_2O, τ_1 = 0.306 ± 0.003 ms (25%) and τ_2 = 1.21 ± 0.01 ms (75%); D_2O, τ_1= 1.10 ± 0.02 ms (25%) and τ_2 = 2.72 ± 0.01 ms (75%)) giving hydration states of q_1 = 2.5 ± 0.5 and q_2 = 0.3 ± 0.5, while for Tb(III) (H_2O, τ_1 = 0.63 ± 0.04 ms (25%) and τ_2 = 1.48 ± 0.03 ms (75%); D_2O, τ_1= 0.97

DOI: 10.1021/ja511799n
J. Am. Chem. Soc. 2015, 137, 1983−1992

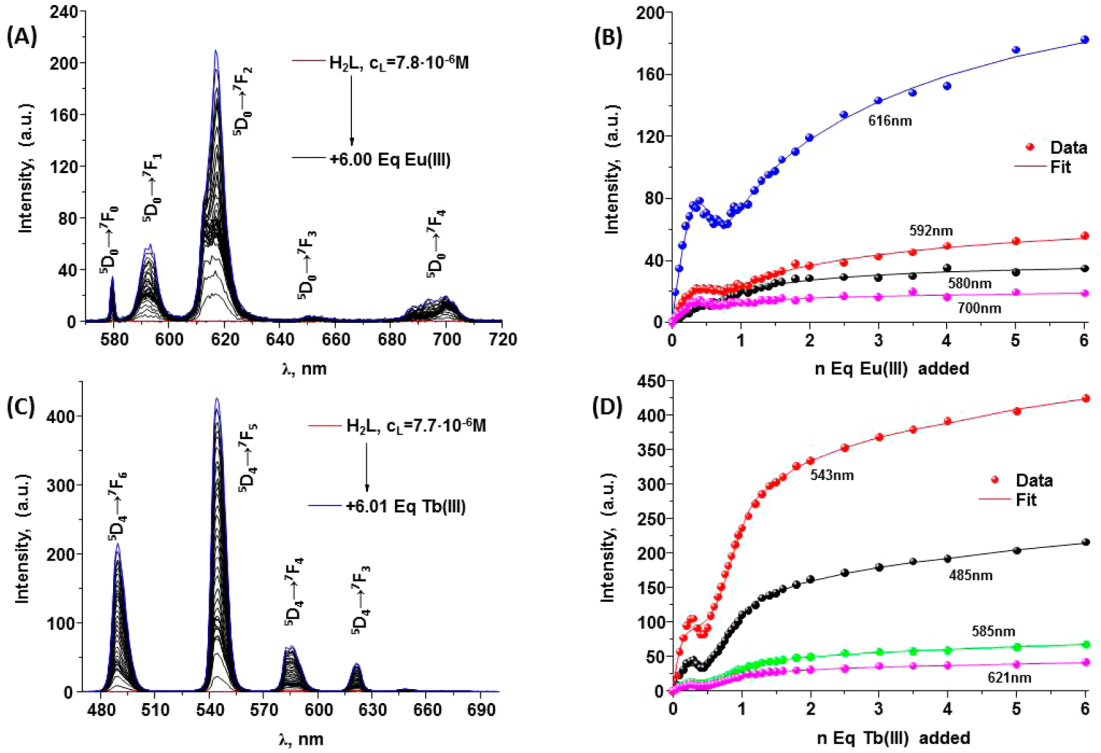

Figure 1. Changes in (A) the Eu(III) centered emission spectra upon titrating $\mathbf{H_2L}$ (7.80×10^{-6} M) with $Eu(CF_3SO_3)_3$ (0 → 6 equiv), (B) experimental binding isotherms (●) and their corresponding fits (—) for the titration with $Eu(CF_3SO_3)_3$, (C) changes in the Tb(III) centered emission spectra upon titrating $\mathbf{H_2L}$ (7.70×10^{-6} M) with $Tb(CF_3SO_3)_3$ (0 → 6 equiv), (D) experimental binding isotherms (●) and their corresponding fits (—) for the titration with $Tb(CF_3SO_3)_3$ in methanol at 298 K.

± 0.03 ms (25%) and τ_2 = 2.12 ± 0.02 ms (75%)) the fits were giving q_1 = 2.5 ± 0.5 and q_2 = 0.7 ± 0.5. These results indicate the formation of both $Eu(\mathbf{H_2L})_3$ and $Tb(\mathbf{H_2L})_3$ in solution as a major component with the possible minor contribution from a second species, namely, $Ln(\mathbf{H_2L})_2(H_2O)_3$, the formation of which can be explained by the dissociation process in the following manner: $Ln(\mathbf{H_2L})_3 \rightarrow Ln(\mathbf{H_2L})_2(H_2O)_3 + \mathbf{H_2L}$. These complexes were soluble in a variety of solvents such as CH_2Cl_2, $CHCl_3$, CH_3CN, and CH_3OH and did not give rise to the formation of soft matter in these solvents.

Photophysical Analysis of the Self-Assembly Formation between $\mathbf{H_2L}$ and Tb(III) or Eu(III) in Solution. The focus here will be mainly on the identification of the species involved in the gelation process reported in this work (see discussion below). We performed the self-assembly studies in the solution between $\mathbf{H_2L}$ and Ln(III) in both CH_3CN (see Supporting Information) and CH_3OH at low concentration. The changes in the absorbance and luminescence spectra were monitored upon addition of $Ln(CF_3SO_3)_3$ to $\mathbf{H_2L}$ solution in methanol (see Supporting Information). The absorption spectrum of $\mathbf{H_2L}$ in CH_3OH consisted of two main bands centered at 235 nm (ε_{235} = 32 070 M^{-1} cm^{-1}) and a longer-wavelength band centered 275 nm (ε_{275} = 6935 M^{-1} cm^{-1}) with a shoulder at 285 nm (ε_{285} = 4096 M^{-1} cm^{-1}). The addition of Eu(III) or Tb(III) to the solution of $\mathbf{H_2L}$ in methanol gave rise to changes in the absorption spectra that were to a great extent identical, where hyperchromism and a red shift were observed for the 235 nm transition (see Supporting Information), while the bands at 275 and 285 nm remained mainly unchanged. The evolution of the Eu(III)- and Tb(III)-centered emissions were monitored as well upon excitation at 275 nm (Figure 1). Here the intensity increased for both systems upon addition of the metal ions demonstrating successful population of the excited states of these ions upon coordination to $\mathbf{H_2L}$; the characteristic emission bands appeared at 580, 595, 616, 650, and 695 nm for Eu(III) (assigned to $^5D_0 \rightarrow {}^7F_J$ (J = 0–4) transitions), while for Tb(III) these bands appeared at 490, 545, 583, and 620 nm (assigned to $^5D_4 \rightarrow {}^7F_J$ (J = 6–3)), Figure 1. For both the emission was gradually enhanced until the addition of ~0.3 equiv of Ln(III). This was followed by a slight decrease for both systems until the addition of ~0.75 equiv, after which the emission grew steadily. The appearance of the strong contribution from the ΔJ = 0 band in the Eu(III) emission spectra would indicate that the 1:3 complex existed dominantly in C_3 symmetry.[17]

The changes in the ground and excited states for both titrations were analyzed by fitting the data using the nonlinear regression analysis program SPECFIT. Factor analysis of the overall changes observed from these titrations suggested the formation of four species and the spectroscopic data changes were satisfyingly fitted to 1:1, 1:2, 2:2, and 3:2 stoichiometries of $\mathbf{Ln:H_2L}$ (see Supporting Information), being unable to get a reliable fit for the formation of 1:3 which is clearly also formed, Figure 1B,D. In the case of the absorption data, it is necessary to take into account the absorbance of the ligand itself, as it was not possible to determine the difference between the presence of 1:1 and 2:2 species; thus, 1:1 was omitted from the binding model. The binding constants found by fitting the changes in absorption spectra for the equilibria with the Eu(III) ion were found as follows: log $\beta_{1:2}$ = 12.2 ± 0.2, log $\beta_{2:2}$ = 18.9 ± 0.4, log $\beta_{3:2}$ = 25.2 ± 0.4. At the same time very similar values were found for the Tb(III) system: log $\beta_{1:2}$ = 12.4 ± 0.4, log $\beta_{2:2}$ = 19.7 ± 0.6, log $\beta_{3:2}$ = 24.0 ± 0.6. Moreover, analysis of the lanthanide centered emission enabled the successful distinction

DOI: 10.1021/ja511799n
J. Am. Chem. Soc. 2015, 137, 1983–1992

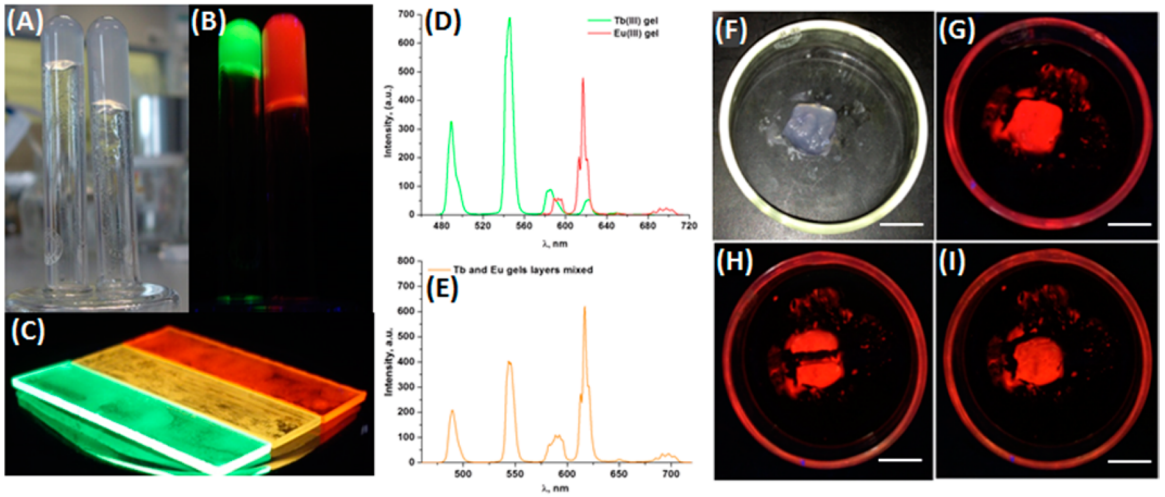

Figure 2. Eu(III) and Tb(III) gels (A) in day light and (B) their luminescence under UV light. (C) Luminescence of Eu(III), Tb(III), and Eu(III)/Tb(III) gels on quartz plates. (D) Eu(III), Tb(III), and (E) Eu(III)/Tb(III) mixed gel luminescence spectra at 25 °C (λ_{ex} = 275 nm). (F–I) Healing experiment of Eu(III) gel with (F) Eu(III) gel in the day light, (G) the same gel under UV light, (H) gel after being cut in half, and (I) self-healing properties of the gel (scale bars, 1 cm).

between 1:1 and 2:2 stoichiometries for Eu(III), with log $\beta_{1:1}$ = 6.7 ± 0.1, log $\beta_{1:2}$ = 12.6 ± 0.1, log $\beta_{2:2}$ = 18.5 ± 0.1, log $\beta_{3:2}$ = 23.3 ± 0.1. Similar binding constants were obtained for the Tb(III) assemblies: log $\beta_{1:1}$ = 6.6 ± 0.1, log $\beta_{1:2}$ = 11.6 ± 0.1, log $\beta_{2:2}$ = 18.7 ± 0.2, log $\beta_{3:2}$ = 22.7 ± 0.2 (see Supporting Information).

For comparison, the titrations were also repeated in CH_3CN solution; here the solvent is of similar polarity to CH_3OH, but aprotic and as such less competitive. Also, the lack of O–H oscillators would result in less quenching. Here, absorption bands were centered at 235 nm (ε_{235} = 65 811 M^{-1} cm^{-1}) and 275 nm (ε_{275} = 13 244 M^{-1} cm^{-1}) with a shoulder 285 nm (ε_{285} = 7028 M^{-1} cm^{-1}). Upon the addition of Ln(III), significantly greater changes occurred to these seen above for CH_3OH, where all the transitions were greatly affected up to the addition of ∼0.3 equiv, before plateauing (see Supporting Information) and signifying the effect of the media on the self-assembly formation, clearly demonstrating the formation of the expected 1:3 stoichiometry. These changes in the absorption spectra were subjected to nonlinear regression analysis. Factor analysis supported the formation of self-assemblies, with stoichiometries of 1:1, 1:2 and 1:3 (**Ln:H_2L**) (see Supporting Information) all being determined. It should be noted that **H_2L** does not show any kinetic inertness toward lanthanide ions in solution compared to the similar **L8** ligand which has no carboxylic groups in its structure.[32] The stability constants[40] for Eu(III) were determined as log $\beta_{1:1}$ = 6.7 ± 0.1, log $\beta_{1:2}$ = 14.2 ± 0.1, and log $\beta_{1:3}$ = 21.0 ± 0.1, while for Tb(III) constants of log $\beta_{1:1}$ = 6.9 ± 0.1, log $\beta_{1:2}$ = 13.8 ± 0.2, and log $\beta_{1:3}$ = 18.7 ± 0.5 were found. These results complement those observed in CH_3OH quite well. For both, the Eu(III) and Tb(III) centered emissions were also "switched on" demonstrating the formation of the lanthanide directed self-assembly in solution, with emission spectra similar to that seen in CH_3OH.[28,41] The analysis of the Ln(III)-centered emission changes also allowed us to determine the binding constants (see Supporting Information). Moreover, here the 1:3 stoichiometry was observed unlike in our analyses in CH_3OH.

NMR Studies of H_2L with La(CF_3SO_3)$_3$. The presence of the 1:1 and 1:2 species was confirmed by mass-spectrometry studies of the complexes (see Supporting Information) while the 1:3 could not be detected. However, the determination of the *q* values above indicated the presence of both the 1:3 and the 1:2 species in the solution, in the ratio of 75:25. With a view to understand the binding mechanism between **H_2L** and Ln(III) ions and for the purposes of elucidating the numbers of species involved in the self-assembly process at higher concentrations, a ^{1}H NMR titration (400 MHz, CD_3OD) was carried out (see Supporting Information) using **H_2L** (c = 1.1 × 10^{-3} M) and the diamagnetic ion La(III) (from La(CF_3SO_3)$_3$). The results (see Supporting Information) demonstrated that, even upon the addition of 0.10 equiv of La(III), significant broadening and downfield shifts were observed for all the ligand protons (the aromatic resonances appearing at 7.45, 7.98, 8.20, and 8.34 ppm), signifying the self-assembly formation, which is best explained as being in a fast exchange on the NMR time scale. The overall titration profile can be viewed in two parts; initially, between the addition of 0.1 → 0.3 equiv of La(III), the protons assigned to the pyridyl unit became particularly broadened, being shifted upfield, while the protons of the benzoic acid were slightly shifted downfield, and only became significantly broadened upon the addition of 0.3 equiv. Between the addition of 0.3 → 1.0 equiv of La(III), the overall changes were best explained as being in slow exchange, where the pyridyl resonances became more broadened and disappeared with growing in of new broad signals assigned to the pyridyl protons further downfield ($\Delta\delta$ ∼ 0.5 ppm). Concomitantly, minor but clear changes were seen for the benzoic acid protons ($\Delta\delta$ ∼ 0.05 ppm). Further additions of La(III) resulted in the formation of a spectrum (after ca. 1.1 equiv) of resolved signals for all the aromatic resonances, centered at 7.53, 8.03, 8.58, and 8.60 ppm. During the titration, methylene bridge protons were in slow exchange, being shifted from 4.71 to 4.92 ppm from 0 → 2 equiv of La(III). These overall changes clearly indicate a stepwise formation of a self-assembly, where the initial formation of the 1:3 stoichiometry occurs, followed by formation of a higher order self-assembly, involving the terminal carboxylic groups which consequently shifts the equilibrium toward the formation of polymeric species. As such, these results confirm what was seen in solution

DOI: 10.1021/ja511799n
J. Am. Chem. Soc. 2015, 137, 1983–1992

at lower concentration in the absorption and the emission titrations above.

Formation of Lanthanide Gels from $Ln(H_2L)_3(CF_3SO_3)_3$. Having demonstrated the formation of a higher order self-assembly in solution, we next turned our attention toward formation of such large supramolecular polymeric self-assembles at higher concentrations, as these would be expected to result in the formation of supramolecular gels.[9−11] Hence, as seen in the ^{1}H NMR titrations, the further addition of Eu(III) or Tb(III) (such as $LnCl_3$, $Ln(ClO_4)_3$, $Ln(CF_3SO_3)_3$, and $Ln(CH_3COO)_3$) would enable us to generate polymeric systems by "cross-linking" the above 1:3 and 1:2 **Ln:H_2L** stoichiometries through bridging of the terminal carboxylic acid groups, as demonstrated schematically in Scheme 1. This involved preparing a ∼10 mM solution of **H_2L** followed by the addition of the corresponding $Ln(CF_3SO_3)_3$ (Ln = Eu and Tb) in a 1:3 **Ln:H_2L** stoichiometry under microwave irradiation at 75 °C for 20 min (see Supporting Information), followed by cooling the solution to room temperature. To this solution were added various stoichiometric ratios of lanthanide salts (relative to **$Ln(H_2L)_3$**), resulting in the formation of clear solutions in all cases, except for $Ln(CH_3COO)_3$. Using $Ln(CH_3COO)_3$ the formation of a soft gel-like precipitate was observed at various (**$Ln(H_2L)_3$:$Ln(CH_3COO)_3$**) stoichiometries after these solutions were subjected to further microwave irradiation at 75 °C. Analysis of the stoichiometric dependences of $Ln(CH_3COO)_3$ showed that upon full coordination (*i.e.* each of the six carboxylates coordinate to a single Ln(III) ion) a clear solution was formed while smaller ratios of **Ln:$(H_2L)_3$:$Ln(CH_3COO)_3$** enabled formation of gel-like precipitates, the use of a 1:0.5 ratio giving rise to the formation of the most stable soft matter. These initial soft self-assembly structures were then subjected to centrifugation (3500 rpm, 10 min), which instantaneously led to the formation of robust gels that were resistant to inversion tests as demonstrated for both the Eu(III) and Tb(III) gels formed in Figure 2A. Similarly, such gels could be formed upon simply storing the samples after microwave irradiation at room temperature overnight; microstructural analysis of both systems indicated the formation of gels with identical morphology. Both gels were slightly opaque (to the naked eye) and were resistant to inversion tests. Furthermore, both were shown to be brightly luminescent upon exposure to UV-light irradiation (Figure 2B). TGA analysis of these Eu(III) and Tb(III) gels (see Supporting Information) showed the weight loss of 98.2 and 98.4 wt % upon heating the samples from 20 °C until 85 °C, which corresponds to the evaporation of the methanol (used to gel these), after which the remaining complex was stable until ∼300 °C when the organic content of the complexes starts to decompose. Thus, both of the obtained lanthanide gels contain ca. 1.7 ± 0.1 wt % of the complex and ∼98.3 ± 0.1 wt % of the methanol.

As alluded to above, these gels were highly luminescent upon UV-light irradiation, Figure 2B; the green and red emission observed was that of Eu(III) and Tb(III), respectively, under excitation at 275 nm as seen in solution studies (Figures 1 and 2D). Both samples were prepared under identical experimental conditions. In the spectra recorded for both samples (Figure 2D), characteristic sharp line-like emission bands were observed at 579, 593, 616, 650, and 696 nm for Eu(III)-gel ($^5D_0 \rightarrow {}^7F_J$, J = 0−4) and at 489, 545, 585, 622 nm for Tb(III)-gel ($^5D_4 \rightarrow {}^7F_J$, J = 6−3). The emission spectra of the gels recorded after transferring them to a quartz slide (Figure 2C) were structurally similar to the emission spectrum obtained for the self-assembly formation in the solution discussed above. However, some minor notable differences were observed for the Eu(III) emission such as the contribution from the $\Delta J = 0$ transition being much less intense, which is an indication of changes in the symmetry of the Eu(III) centers upon gelation. As discussed above, the luminescence quantum yields for both complexes were shown to be similar for both the Eu(III) and Tb(III) complexes. Consequently, the luminescence intensity for their corresponding gels was similar.

This enabled us to form a new gel by simply mixing (mechanically) equal volumes of the two Ln(III) gels, which resulted in formation of a new yellow-orange luminescent Eu(III)/Tb(III) gel (Figure 2C,E), the emission spectrum of which showed the two main emission bands occurring at 545 (Tb(III) emission) and 616 nm (Eu(III) emission), Figure 2E. This color corresponds to coordinates of (0.47, 0.47) on a CIE diagram (see Supporting Information). Various experiments were carried out to investigate the mixing of these two emissive gels and the formation of a new luminescent gel. For instance, first forming **Eu:H_2L** or **Tb:H_2L** complexes in solution and treating these with $Tb(CH_3COO)_3$ and $Eu(CH_3COO)_3$, respectively, led to the formation of luminescent gels, which, unlike these seen for the 1:1 mixing of the gels discussed above, had different emission colors. The latter indicated the contribution that the bridging lanthanide ion (*i.e., via* the carboxylate groups) had on the luminescent properties of the soft matter and the ability of the ligand to sensitize the ions at the two different binding units within **H_2L** (see Supporting Information). The difference in the emission from these mixed gels can also be explained by mapping the colors on to the CIE diagram (see Supporting Information), as above.

Healable Properties of Lanthanide Gels. The above supramolecular gels represent systems that are in constant nonequilibrium self-assembly processes, which can lead to features such as self-healing. Self-healing materials are of great current interest across the scientific community,[14,20−24] particularly as such materials can mimic naturally occurring biopolymers. While self-healing materials have been known for the past few decades, they are generally made of cross-linked polymers (such as hydrogels).[42,43] However, such systems often have limited lifespans, where unexpected damage from constant strain and stress can result in degradation of the materials. Since both the Eu(III) and Tb(III) gels are formed through a dynamic process, where the recognition of 1:2 or the 1:3 **Ln:H_2L** complexes by the second lanthanide ion at the carboxylic acid terminus gives rise to a three-dimensional coordination network, as depicted in Scheme 1, we foresaw that both could potentially function as self-healing materials. As the formation of the gel is induced by the binding of Ln(III) to **H_2L** which follows fast kinetics, we anticipate that the self-healing process will follow a similar trend. Indeed, the excess number of free carboxylic acid groups from the ligands and high coordination number of the lanthanides will ensure self-healing of the gel through coordination. The results from our analysis are shown in Figure 2F−I, using the Eu(III) gel formed as discussed above. The gel was cut in two, and reassembled instantaneously without external stimuli through self-healing; the red emission from the gel clearly aided in the visual observation of the healing properties. Similarly, the Tb(III) gels exhibited self-healing properties (see figure in abstract). The images (Figure 2G,I) show that even to the naked eye these look similar despite the former being an example of an uncut

DOI: 10.1021/ja511799n
J. Am. Chem. Soc. 2015, 137, 1983−1992

gel, while the latter is the same gel after having been cut and then spliced together again (*cf.*, Figure 2H). In fact, it is clear that the two parts have interacted together in such a manner that the cut itself is no longer visible; *i.e.*, a splicing of two mechanically and physically identical gel parts results in healing. This could indicate that within the gel structure the diffusion of the solvent and hence interaction of the lanthanide ions with the carboxylic groups between the edges of the cut is rapid. Consequently, the healing process, which one would expect to be taking place at the carboxylic terminus (as discussed above), through host−guest interactions where the lanthanide is coordinating to free carboxylates and as such functioning within this system as supramolecular glue, is homogeneous over the surface of the cut. Similar effects were seen for the Tb(III) samples (see Supporting Information and figure in abstract), where the cut was healed and not visible to the naked eye. In contrast to this, we also spliced together the Eu(III) and the Tb(III) gels. The images from that experiment (see Supporting Information and figure in abstract) also demonstrated that interaction between the two gels occurred. However, it was not clear that inner diffusion of ions between the two parts was occurring, as this would be expected to give rise to an orange gel as we had demonstrated above by mechanically mixing the two. Nevertheless, a slight yellow emission could be seen within the border of the cut. This would suggest that either this is due to reflection of light, or that while the host−guest interaction is, in principle, the same, then at molecular level the dynamic flow of ions between the two materials is different, possibly being hindered by macroscopic properties of the gels, such as its density, fibrous nature, *etc.* and, hence, their rheological properties. With a view to probing these self-healing properties further, we next carried out both morphological and rheological analysis of the three gel types shown in Figure 2C.

Morphological Properties of Eu(III) and Tb(III) Gels. The morphology of the gels was investigated using scanning electron microscopy (SEM) that gave a high surface signal on samples that were drop cast and dried on silica plates. The results from this analysis are shown in parts A−C for the three gels imaged (see more images in Supporting Information). The SEM images in Figure 3, at first instance show gels possessing similar morphology. All display fibrous nature with an average width of the fibers being ∼30−50 nm, consisting of long intertwining bundles of strings that are packed into strands, which overlap with each other, giving rise to "cotton- or noodle-like" material. This would be expected, given the use of the same ligand for all and the only difference between them being the nature of the lanthanide. However, closer examination of these images clearly demonstrated that the three gels are of different morphology, as the Tb(III) gel SEM images are shown to be significantly more tightly packed in comparison to that seen for Eu(III). For the latter, the packing of the fibrous structure is significantly more porous. This kind of imaging was carried out on several different samples all of which had been aged under identical conditions, and all gave identical results. This supports our earlier finding, that the macroscopic structure of the two gels previously shown in Figure 2B is different, even though they were made under identical experimental conditions (i.e., same concentration, volume, *etc.*), but they clearly have different volume, despite the fact that the solvent content was determined to be of the same for both using TGA analysis. This could indicate that, for the two different systems, the Eu(III) and Tb(III) supramolecular polymers formed, as depicted in Scheme 1B, interact differently

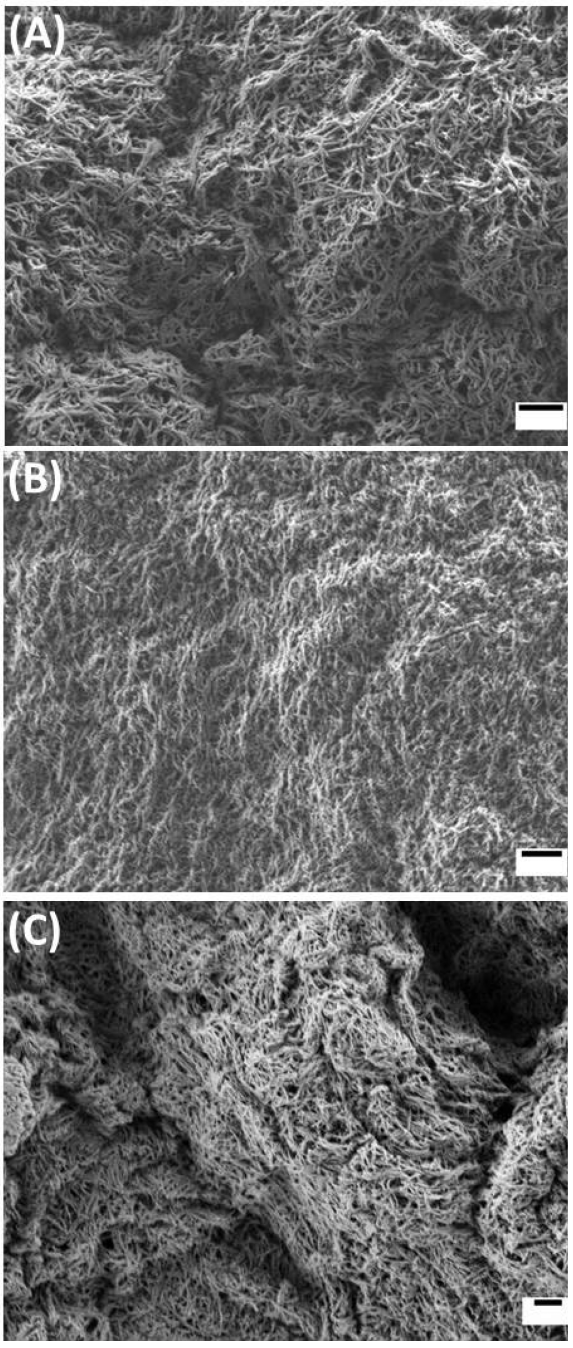

Figure 3. SEM images of (A) Eu(III), (B) Tb(III), and (C) Eu(III)/Tb(III) mixed gels dried on the silicon plates (scale bars, 500 nm).

with the solvent in the gelation process. This was further confirmed by the SEM images of the mechanically mixed Eu(III)/Tb(III) gel, as these images show different morphology to these of the individual gels, as for the mixed gel the packing and porosity seem to be different. This result is in line with what would be expected for the formation of new soft matter from starting materials possessing different morphological properties. It would also support our observation above that the homosupramolecular polymers heal differently from these seen when the two were spliced together. To probe this further we carried out rheological analysis of these three gels.

Rheology. With the aim of knowing the mechanical properties of these novel metallogels, rheological studies (strain

DOI: 10.1021/ja511799n
J. Am. Chem. Soc. 2015, 137, 1983−1992

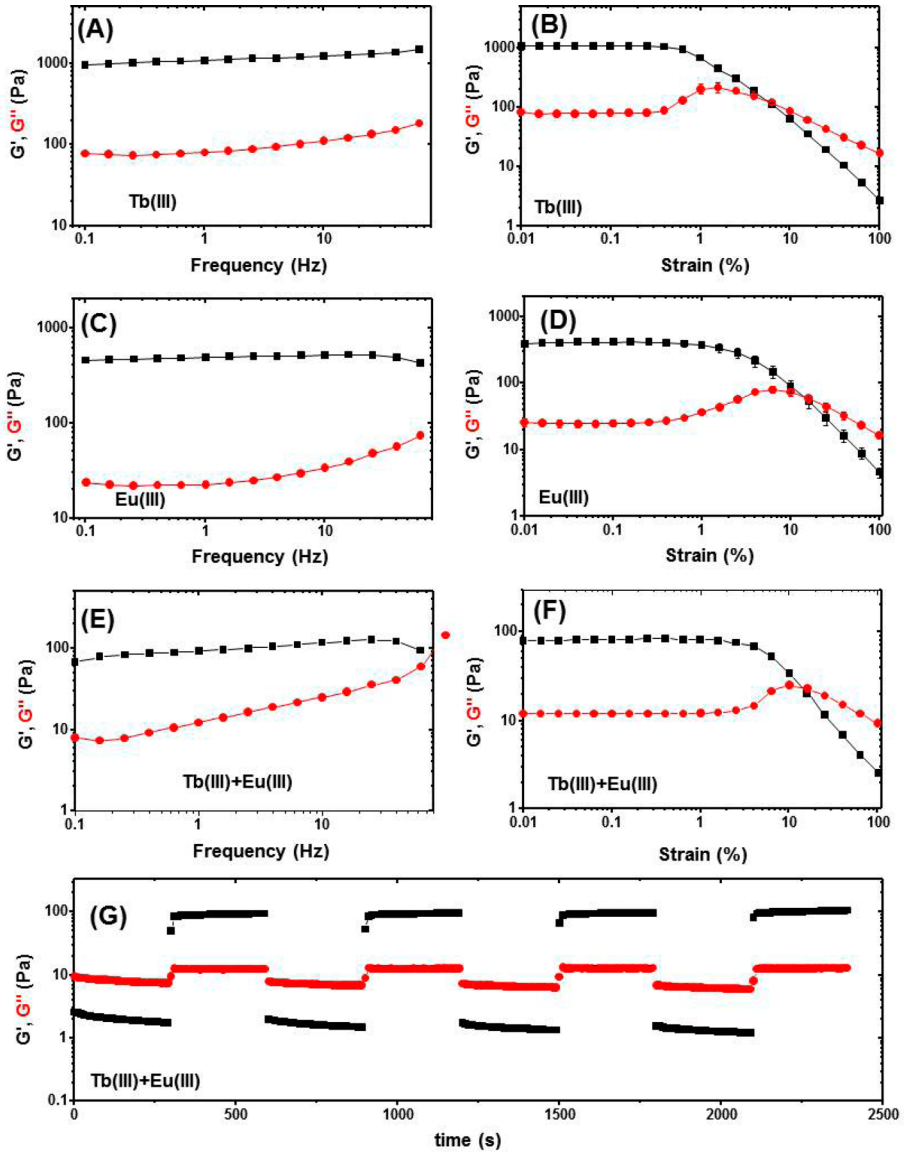

Figure 4. Oscillatory rheology measurements of lanthanide gels. Frequency dependence of the storage modulus G' (■) and loss modulus G'' (●) at a strain amplitude of 0.1% are shown: (A) Tb(III), (C) Eu(III), and (E) Eu(III)/Tb(III). The corresponding strain sweeps at f = 1 Hz for (B) Tb(III), (D) Eu(III), and (F) Eu(III)/Tb(III) are also displayed. Panel G shows the recovery test for Eu(III)/Tb(III). By applying alternating strain amplitudes of 100% and 0.1% at f = 1 Hz the response changes from liquid- to solid-like, respectively. The moduli in these regimes remain unchanged.

and frequency sweeps) were performed, showing that the viscoelastic properties of the three gels shown in Figure 4 are like these commonly seen for a cross-linked polymer network. Note that all the data shown in Figure 4A–F were averaged over three consecutive runs on the same sample. There is little frequency dependence of the moduli in the linear viscoelastic regime for both the Tb(III) and Eu(III) gels (Figure 4A,C), and their response is solid-like ($G' > G''$). The mixed Eu(III)/Tb(III) gel exhibits similar behavior except that G'' approaches G' at high frequencies indicating a crossover to a liquid-like regime. The corresponding strain sweeps for the three gels are shown in Figure 4B,D,F. At low strain amplitudes, the response is solid-like; the storage modulus remains constant until the yield strain is reached at which point the gel starts to flow and G' decreases. While the overall behavior is similar for the three gels, the Eu(III)/Tb(III) gel is noticeably softer compared to the pure Tb(III) and Eu(III) gels. The latter have storage moduli of 1.10 and 0.41 kPa in the linear regime, respectively, while G' for the mixture is 0.08 kPa, an order of magnitude smaller compared to the pure gels. Moreover, the yield strains for Tb(III) and Eu(III) are around 0.5% while Eu(III)/Tb(III) gel yields at 1.5%. The remarkable reproducibility is indicated by the small error bars in Figure 4A–F. We also tested the recovery properties of the gels by imposing alternating strain amplitudes of 100% and 0.1% at a constant 1 Hz oscillation frequency.[44] As shown in Figure 4G the Eu(III)/Tb(III) gel went from liquid-like ($G'' > G'$) to solid-like ($G' > G''$) behavior almost instantly with a quick recovery of the original values of the moduli in these two regimes. The same behavior was observed for both the original Eu(III) and the Tb(III) gels (see Supporting Information). These results point to the formation of stronger "pure" Eu(III) and Tb(III) gels if we compare G' and G'' values with those obtained for the Eu(III)/Tb(III) mixture gel. This could be due to a self-recognition

DOI: 10.1021/ja511799n
J. Am. Chem. Soc. 2015, 137, 1983–1992

process occurring in the "pure" gels that is not happening in the same way when the gels are mixed which could explain the lower values obtained in these experiments.

These are somewhat unexpected rheological results, given the fact that the ligand is the same for all three cases, and that Eu(III) and Tb(III) display binding affinity for the formation of **Eu:H_2L** and **Tb:H_2L** complexes in solution that are almost identical for both systems. Hence, the difference seen in the rheology has to be due to the effect of the lanthanide ion itself, and how these ions function as bridges in the formation of the supramolecular polymer at higher concentration. This could explain the differences seen in the SEM imaging above, where the packing of the fibers in the Eu(III) gel is less dense than that seen in the Tb(III) gel, where both are then different from that seen for the mixed gel. It has to be noted that both Eu(III) and Tb(III) gels heal. While healing is also observed for the mixed gel the supramolecular interaction is different as indicated by their rheological properties and in the analysis of their morphology. Hence, these unexpected rheological results demonstrate that slight differences in the electron configuration of similar lanthanides ions can have a significant effect on the supramolecular level when the two gels interact with each other.

CONCLUSIONS

In this work we have developed a new method for the preparation of luminescent Ln(III) directed self-assembly gels from the Eu(III) and Tb(III) complexes obtained with the dipicolinic acid derived ligand **H_2L**, from which we formed Eu(III), Tb(III), and mixed Eu(III)/Tb(III) gels. The self-assembly studies of the individual complexes was explored in CH_3CN solution, from which we determined various species; however, different speciation was found in the same experiments when performed in CH_3OH, where the role of the carboxylic acid groups became apparent as these were involved in coordination to the lanthanides, providing the platform necessary for the formation of a coordinating polymer. The driving force for the formation of the gel is the interaction between the ligand and metal ions unlike in the case of the gels based on organic molecules only, which are obtained through hydrogen bonds, $\pi-\pi$ stacking, and dipole−dipole interactions.[1−4] Thus, the response to the internal stimuli between these two classes of gels will be different. Here we generated supramolecular polymers, by using Eu(III) or Tb(III) complexes, formed under microwave conditions in 1:3 stoichiometry, followed by treatment with acetate salts of Eu(III) or Tb(III). This gave luminescent gels, emitting with characteristic red or green lanthanide based emission. Imaging of the gels by SEM showed similarity in the morphology of both gels having a "cotton-like" fibrous microstructure, but with different porosity; the Tb(III) exhibited higher density of fibers packing. Similarly, a mixed Eu(III)/Tb(III) gel was formed, which had different morphological features to the individual "pure" gels. This fact was confirmed by rheological studies, which showed that differences existed between all of the three gels, a consequence of the supramolecular interactions between the lanthanide ions and the complexes in the gelation process. These results clearly demonstrated the important role of host−guest interactions in such gel formation. These gels showed the characteristics of self-healing, demonstrated by the recovery to the same value of G' as the one observed at the start within less than 30 s, even in the case of a mixture of the original Eu(III) and Tb(III) gels. Remarkably, the self-healing process of the "pure" gels was significantly different from the mixed Eu(III)/Tb(III) gel underlining the significance of the Ln(III) recognition processes occurring during self-healing.

EXPERIMENTAL SECTION

Materials and Methods. All solvents and chemicals were purchased from commercial sources and used without further purification. Deuterated solvents used for NMR analysis (CD_3CN, CD_3OD, $(CD_3)_2SO$) were purchased and used as received.

The ^{1}H NMR spectra were recorded at either 400 or 600 MHz instruments. All ^{13}C NMR spectra were recorded at either 100 or 150.9 MHz. Chemical shifts are reported in ppm with the deuterated solvent as the internal reference. All NMR spectra were carried out at 293 K.

Mass spectrometry was carried out using HPLC grade solvents using either electrospray mass spectrometer (ESI) or by using Maldi-Q-TOF mass spectrometer. High resolution ESI mass spectra were determined relative to a standard of leucine enkephaline, while high resolution Maldi-Q-TOF spectra were analyzed using Glu-Fib with an internal reference peak of m/z 1570.6774.

Infrared spectra were recorded on a spectrometer equipped with universal ATR sampling accessory.

Thermal gravimetric analysis was performed on an instrument equipped with an ultramicrobalance with a sensitivity of 0.1 μg. The temperature range is from 20 to 800 °C with a scan rate 10 °C/min.

X-ray data (Supporting Information Table S1) was collected using a diffractometer with a graphite-monochromated Mo Kα radiation (λ = 0.710 73 Å). A suitable crystal was selected and mounted on a 0.3 mm quartz fiber tip and placed on the goniometer head in a 150 K N_2 gas stream. The data sets were collected using Crystalclear-SM 1.4.0 software. Space group determination was obtained using Crystalstructure ver.3.8 software. The structure was solved by direct methods (SHELXS-97) and refined against all F^2 data (SHELXL-97).[45] All H atoms, except for N−H protons, were positioned geometrically and refinied using a riding model with d(CHaro) = 0.95 Å, U_{iso} = 1.2U_{eq} (C) for aromatic and 0.98 Å, U_{iso} = 1.2U_{eq} (C) for CH_3. N−H protons were found from the difference map and either freely refined or fixed to the attached atoms with UH = 1.2UN. CCDC 1019596 contains the supplementary crystallographic data for this paper. These data can be obtained free of charge from The Cambridge Crystallographic Data Centre via www.ccdc.cam.ac.uk/data_request/cif.

Photophysical Measurements. Unless otherwise stated, all measurements were performed at 298 K in methanol (HPLC grade) and acetonitrile (spectroscopic grade) solutions. The stock solutions of **H_2L** in acetonitrile were prepared using 4% of chloroform (spectroscopic grade). UV−vis absorption spectra were measured in 1 cm quartz cuvettes. Baseline correction was applied for all spectra. Emission (fluorescence, phosphorescence, and excitation) spectra and lifetimes were recorded at 298 K by using a thermostated unit block. Phosphorescence lifetimes of the Eu($^5D_0$) and Tb($^5D_4$) excited states were measured in both water and deuterated water and methanol and deutarated methanol in time-resolved mode at 298 K. They are averages of three independent measurements, which were made by monitoring the emission decay at 616 and 543 nm, which corresponds to the maxima of the Eu(III) $^5D_0 \rightarrow {}^7F_2$ and to the $^5D_4 \rightarrow {}^7F_J$ Tb(III) transitions, respectively, enforcing a 0.1 ms delay.

The quantum yields ($Q_{rel}^{Eu,L}$) were measured by relative method[46,47] using $Cs_3[Eu(dpa)_3]\cdot 9H_2O$ complex in 0.1 M Tris buffer (pH = 7.45) (Q_{abs}^{Eu} = 24.0 ± 2.5%)[38] as a standard with known quantum yield, to which the absorbance and emission intensity of the sample are compared according to

$$Q_{rel}^{Eu,L} = \frac{Q_x}{Q_r} = \frac{E_x}{E_r} \times \frac{A_r(\lambda_r)}{A_x(\lambda_x)} \times \frac{I_r(\lambda_r)}{I_x(\lambda_x)} \times \frac{n_x^2}{n_r^2} \quad (1)$$

where subscript r is reference and x is sample. The other abbreviations are as follows: E, integrated luminescence intensity; A, absorbance at the excitation wavelength; I, intensity of the excitation light at the

DOI: 10.1021/ja511799n
J. Am. Chem. Soc. 2015, 137, 1983−1992

same wavelength; *n*, refractive index of the solution. The estimated error for quantum yields is ±10%.

Spectrophotometric Titrations and Binding Constants. The formation of the luminescent (**M:H_2L**, where M = metal and **H_2L** = dipicolinic based dicarboxylic ligand) species was ascertained by both UV−vis and luminescence titrations of a solution of **H_2L** (~1×10^{-5} M) with **$M(CF_3SO_3)_3 \cdot 6H_2O$** (M = Eu(III), Tb(III)) (0 → 6 equiv) at 298 K. The data were fitted using the nonlinear regression analysis program, SPECFIT.[40,48] Each titration was repeated with evaluation of the binding constants values for at least three times until data convergence was achieved.

Microscopy Studies of the Gels. To image the gel samples by scanning electron microscopy (SEM), they were deposited manually onto clean silicon samples with a thick silicon dioxide layer. The spatula and glass pipettes used for dosing and silicon pieces used as substrates were all cleaned thoroughly by sonication in HPLC grade acetone followed by HPLC grade propan-2-ol. All components were dried in two steps using a high pressure nitrogen gun and further dried under ambient conditions. The gels were manually drop cast on to the silicon at room temperature and dried over 5 days at ambient conditions. The samples prepared for the imaging using SEM did not have any additional conductive layer cover.

Rheological Studies of the Gels. The rheology of the gels was measured with a rheometer and a 50 mm parallel plate geometry. After placing the sample, the upper plate was slowly lowered until a gap of size 0.5 mm was reached. Any residual stresses inside the samples that built up during loading were relieved by gentle preshearing. We performed several oscillatory strain sweeps until the normal force equilibrated before the measurements commenced. During the oscillatory measurements, the normal force did not change appreciably and was always below 0.09 N. These samples were kept at a constant temperature of 20 °C. A solvent trap was used to avoid the evaporation of methanol during the measurements. The oscillatory strain sweep measurements were performed at a frequency of 1 Hz while the frequency sweeps were performed at a constant strain amplitude of 0.1%. All the data were averaged over three consecutive runs.

■ ASSOCIATED CONTENT

Ⓢ Supporting Information

NMR, X-ray, HR-MS, TGA, and the photophysical investigations for each system studied, including absorption, fluorescence, phosphorescence, and excitation spectra as well as the tables containing the different fits performed to determine binding constants; healing studies; CIE diagram; morphology, and rheology studies. Crystal data in CIF format. This material is available free of charge via the Internet at http://pubs.acs.org.

■ AUTHOR INFORMATION

Corresponding Author

gunnlaut@tcd.ie

Present Address

[‖]Departamento de Química Orgánica and Centro Singular de Investigación en Química Biolóxica e Materiais Moleculares (CIQUS), Universidade de Santiago de Compostela, 15782 Santiago de Compostela, Spain.

Author Contributions

[⊥]These authors contributed equally to this work.

Notes

The authors declare no competing financial interest.

■ ACKNOWLEDGMENTS

We thank University of Dublin and CRANN for their support. This research was supported by the Irish Research Council for Science, Engineering & Technology (IRCSET; postdoctoral fellowship to O.K.) and Science Foundation Ireland (SFI) for RFP Grants and PI Awards. We thank Dr. Steve Comby for the help with CIE diagrams and Dermot Daly for the help with SEM images (AML, CRANN, TCD).

■ REFERENCES

(1) (a) Aida, T.; Meijer, E. W.; Stupp, S. I. *Science* **2012**, *335*, 813−817. (b) Fleming, S.; Ulijn, R. V. *Chem. Soc. Rev.* **2014**, *43*, 8150−8177. (c) Zhao, F.; Lung, M. M.; Xu, B. *Chem. Soc. Rev.* **2009**, *38*, 883−891.

(2) Wang, D.; Tong, G.; Dong, R.; Zhou, Y.; Shen, J.; Zhu, X. *Chem. Commun.* **2014**, *50*, 11994−12017.

(3) Boekhoven, J.; Poolman, J. M.; Maity, C.; Li, F.; van der Mee, L.; Minkenberg, C. B.; Mendes, E.; van Esch, J. H.; Eelkema, R. *Nat. Chem.* **2013**, *5*, 433−437.

(4) Stupp, S. I.; Palmer, L. C. *Chem. Mater.* **2014**, *26*, 507−518.

(5) Terech, P.; Weiss, R. G. *Chem. Rev.* **1997**, *97*, 3133−3159.

(6) Estroff, L. A.; Hamilton, A. D. *Chem. Rev.* **2004**, *104*, 1201−1217.

(7) (a) Esch, J. H. *Langmuir.* **2009**, *25*, 8392−8394. (b) Andrews, P. C.; Junk, P. C.; Massi, M.; Silberstein, M. *Chem. Commun.* **2006**, 3317−3319.

(8) Korevaar, P. A.; George, S. J.; Markvoort, A. J.; Smulders, M. M.; Hilberts, P. A. J.; Schenning, A. P. H.; De Greef, F. A.; Meijer, E. W. *Nature* **2012**, *481*, 492−497.

(9) Buerkle, L. E.; Rowan, S. J. *Chem. Soc. Rev.* **2012**, *41*, 6089−6102.

(10) Tam, A.Y.-Y.; Yam, V.W.-W. *Chem. Soc. Rev.* **2013**, *42*, 1540−1567.

(11) Zhang, J.; Su, C.-Y. *Coord. Chem. Rev.* **2013**, *257*, 1373−1408.

(12) Kumar, D. K.; Steed, J. W. *Chem. Soc. Rev.* **2014**, *43*, 2080−2088.

(13) Banerjee, S.; Kandanelli, R.; Bhowmik, S.; Maitra, U. *Soft Matter* **2011**, *7*, 8207−8215.

(14) Fiore, G.; Rowan, S. J.; Weder, C. *Chem. Soc. Rev.* **2013**, *42*, 7278−7288.

(15) Tam, A. Y.-Y.; Yam, V. W.-W. *Chem. Soc. Rev.* **2013**, *42*, 1540−1567.

(16) Strassert, C. A.; Chien, C.-H.; Galvez Lopez, M. D.; Kourkoulos, D.; Hertel, D.; Meerholz, K.; De Cola, L. *Angew. Chem., Int. Ed.* **2011**, *50*, 946−950.

(17) Eliseeva, S. V.; Bünzli, J.-C. G. *Chem. Soc. Rev.* **2010**, *39*, 189−227.

(18) Kotova, O.; Daly, R.; dos Santos, C. M. G.; Boese, M.; Kruger, P. E.; Boland, J. J.; Gunnlaugsson, T. *Angew. Chem., Int. Ed.* **2012**, *51*, 7208−7212.

(19) Daly, R.; Kotova, O.; Boese, M.; Gunnlaugsson, T.; Boland, J. J. *ACS Nano* **2013**, *7*, 4838−4845.

(20) Harada, A.; Takashima, Y.; Nakahata, M. *Acc. Chem. Res.* **2014**, *47*, 2128−2140.

(21) Qi, Z.; Schalley, C. A. *Acc. Chem. Res.* **2014**, *47*, 2222−2233.

(22) Yu, X.; Chen, L.; Zhang, M.; Yi, T. *Chem. Soc. Rev.* **2014**, *43*, 5346−5371.

(23) Nakahata, M.; Takashima, Y.; Yamaguchi, H.; Harada, A. *Nat. Commun.* **2011**, DOI: 10.1038/ncomms1521.

(24) Mckee, J. R.; Appel, E. A.; Seitsonen, J.; Kontturi, E.; Scherman, O.; Ikkala, O. *Adv. Funct. Mater.* **2014**, *24*, 2706−2713.

(25) Kitchen, J. A.; Barry, D. E.; Mercs, L.; Albrecht, M.; Peacock, R. D.; Gunnlaugsson, T. *Angew. Chem., Int. Ed.* **2012**, *51*, 704−708.

(26) Comby, S.; Stomeo, F.; McCoy, C. P.; Gunnlaugsson, T. *Helv. Chim. Acta* **2009**, *92*, 2461−2473.

(27) Lincheneau, C.; Leonard, J. P.; McCabe, T.; Gunnlaugsson, T. *Chem. Commun.* **2011**, *47*, 7119−7121.

(28) Leonard, J. P.; Jensen, P.; McCabe, T.; O'Brien, J. E.; Peacock, R. D.; Kruger, P. E.; Gunnlaugsson, T. *J. Am. Chem. Soc.* **2007**, *129*, 10986−10987.

(29) Shavaleev, N. M.; Eliseeva, S. V.; Scopelliti, R.; Bünzli, J.-C. G. *Chem.—Eur. J.* **2009**, *15*, 10790−10802.

(30) Di Pietro, S.; Imbert, D.; Mazzanti, M. *Chem. Commun.* **2014**, *50*, 10323−10326.

DOI: 10.1021/ja511799n
J. Am. Chem. Soc. 2015, 137, 1983−1992

(31) Bradberry, S. J.; Savyasachi, A. J.; Martinez-Calvo, M.; Gunnlaugsson, T. *Coord. Chem. Rev.* **2014**, *273*−*274*, 226−241.
(32) Le Borgne, T.; Bénech, J.-M.; Floquet, S.; Bernardinelli, G.; Aliprandini, C.; Bettens, P.; Piguet, C. *Dalton Trans.* **2003**, 3856−3868.
(33) Vermonden, T.; de Vos, W. M.; Marcelis, A. T. M.; Sudhölter, E. J. R. *Eur. J. Inorg. Chem.* **2004**, 2847−2852.
(34) Vermonden, T.; van Steenbergen, M. J.; Besseling, N. A. M.; Marcelis, A. T. M.; Hennink, W. E.; Sudhölter, E. J. R.; Cohen Stuart, M. A. *J. Am. Chem. Soc.* **2004**, *126*, 15802−15808.
(35) Andres, J.; Chauvin, A.-S. *Inorg. Chem.* **2011**, *50*, 10082−10090.
(36) Vázquez, M.; Fabbrizzi, L.; Taglietti, A.; Pedrido, R. M.; González-Noya, A. M.; Bermejo, M. R. *Angew. Chem., Int. Ed.* **2004**, *43*, 1962.
(37) Ali, M. A.; Mirza, A. H.; Ejau, W. B.; Bernhardt, P. V. *Polyhedron.* **2006**, *25*, 3337.
(38) Chauvin, A.-S.; Gumy, F.; Imbert, D.; Bünzli, J.-C. G. *Spectrosc. Lett.* **2004**, *37*, 517−532; Erratum *Spectrosc. Lett.* **2007**, *40*, 193.
(39) Beeby, A.; Clarkson, I. M.; Dickins, R. S.; Faulkner, S.; Parker, D.; Royle, L.; de Sousa, A. S.; Williams, J. A. G.; Woods, M. *J. Chem. Soc., Perkin Trans. 2.* **1999**, 493−503.
(40) Gampp, H.; Maeder, M.; Meyer, C. J.; Zuberbühler, A. D. *Talanta* **1986**, *33*, 943−951.
(41) Hua, K. N. T.; Xu, J.; Quiroz, E. E.; Lopez, S.; Ingram, A. J.; Johnson, V. A.; Tisch, A. R.; de Bettencourt-Dias, A.; Straus, D. A.; Muller, G. *Inorg. Chem.* **2012**, *51*, 647−660.
(42) Appel, E. A.; del Barrio, J.; Jun Loh, X.; Scherman, O. A. *Chem. Soc. Rev.* **2012**, *41*, 6195−6214.
(43) Brantley, J. N.; Wiggins, K. M.; Bielawski, C. W. *Angew. Chem., Int. Ed.* **2013**, *52*, 3806−3808.
(44) Wang, Q.; Mynar, J. L.; Yoshida, M.; Lee, E.; Lee, M.; Okuro, K.; Kinbara, K.; Aida, T. *Nature* **2010**, *463*, 339−343.
(45) Sheldrick, G. M. *Acta Crystallogr., Sect. A* **2008**, *A64*, 112−122.
(46) de Sá, G. F.; Nunez, L.; Wang, Z. M.; Choppin, G. R. *J. Alloys Compd.* **1993**, *196*, 17−23.
(47) Demas, J. N.; Crosby, G. A. *J. Phys. Chem.* **1971**, *75*, 991−1024.
(48) Gampp, H.; Maeder, M.; Meyer, C. J.; Zuberbühler, A. D. *Talanta* **1985**, *32*, 95−101.

DOI: 10.1021/ja511799n
J. Am. Chem. Soc. 2015, 137, 1983−1992